Two-dimensional spin-flop transition in $CoCl_2$-graphite intercalation compounds

K. Y. Szeto and S. T. Chen
Department of Physics, Massachusetts Institute of Technology, Cambridge, Massachusetts 02139

G. Dresselhaus
Francis Bitter National Magnet Laboratory, Massachusetts Institute of Technology, Cambridge, Massachusetts 02139

(Received 15 July 1985)

Two field-dependent susceptibility anomalies are observed in the quasi-two-dimensional spin system of $CoCl_2$-intercalated graphite. These anomalies are explained with use of the Landau free-energy functional applied to the magnetic Hamiltonian of $CoCl_2$-intercalated graphite. In the stage-1 compound, the low-field anomaly at $H_{AS}(T)\approx 160$ Oe is a signature of a two-dimensional antiferromagnetic-spin-flop first-order transition, while the anomaly at a higher field $H_{SF}(T)\approx 300$ Oe is a signature of a spin-flop-ferromagnetic second-order transition. The low-temperature properties of these three phases are analyzed using the transfer matrix method for their c-axis ordering. A comparison of the model calculation and the experimental data indicates that the antiferromagnetic coupling between $CoCl_2$ layers and the sixfold in-plane anisotropy are approximately 160 and 10 Oe, respectively, for the stage-1 compound.

I. INTRODUCTION

Multicritical phenomena in magnetic systems have attracted much attention recently. The most notable examples are MnF_2 (Ref. 1) and $GdAlO_3$ (Ref. 2). The experimental studies of these materials have stimulated a vast amount of theoretical research, such as the investigation of the critical properties near the Lifshitz point.[3,4] Therefore, it is interesting to explore the magnetic properties of new materials in lower dimensions, where the physics is simpler.

Recent interest in the magnetic properties of graphite intercalation compounds (GIC's) (Ref. 5) suggest that these compounds are good candidates for fundamental research on magnetic critical phenomena. The theoretical interest in $CoCl_2$ GIC's stems from the approximate XY nature of the Hamiltonian of $CoCl_2$ (Ref. 5) and the experimental interest from the ability to control the spatial dimensionality in GIC's by controlling the stage of the compounds. The investigation of the Kosterlitz-Thouless transition in this system and the connection to the José, Kadanoff, Kirkpatrick, and Nelson (JKKN) (Ref. 6) model has been reported earlier.[5] It was found that the antiferromagnetic interplanar coupling plays an important role in the magnetic order of $CoCl_2$ GIC's at low temperature.[7,8]

In this paper, we report the experimental measurement of the magnetic differential susceptibility $\chi_{||}$ at a finite in-plane field H_1 (H_1 is applied in the c plane and the probing field of 0.3 Oe is applied parallel to H_1). These field-dependent measurements of the susceptibility at fixed temperature provide a sensitive probe of the magnetic order at low temperature. Two new field-induced anomalies in the susceptibility of a stage-1 $CoCl_2$ GIC are reported.

The experimental data on the magnetic field profile of the susceptibility can be understood in terms of two phase transitions: (i) A first-order transition from an antiferromagnetic phase to a spin-flop phase at a critical field H_{AS}, and (ii) a second-order transition from a spin-flop phase to a ferromagnetic phase at a critical field $H_{SF} > H_{AS}$. The qualitative features of the experimental data can be understood in terms of a Landau free-energy functional, the analysis of which reveals the three phases: an antiferromagnetic phase at low field, a spin-flop phase at intermediate field, and a ferromagnetic phase at high field. The low-temperature properties of these phases have been studied using the transfer-matrix method. The theoretical calculations are in qualitative agreement with the experimental data. The susceptibility anomalies can be explained by a Landau-type model in terms of a competition between two symmetry-breaking fields as well as the effect of the antiferromagnetic interplanar coupling. The experimental work, as well as the theoretical modeling, provide a new system for studies of multicritical phenomena.

In Sec. II we report the discoveries of two field-induced susceptibility anomalies in a stage-1 $CoCl_2$ GIC. From these measurements an experimental phase diagram is obtained. In Sec. III a Landau free-energy functional based on the magnetic Hamiltonian of $CoCl_2$ GIC's (Refs. 5 and 7) is written down and discussed for its possible ground state. A low-temperature analysis using the method of the transfer matrix is given in Sec. IV. Finally, in Sec. V the interpretation of the experimental results of Sec. II for the field-induced susceptibility anomalies is presented in terms of the theory given in Secs. III and IV.

II. FIELD-DEPENDENCE MEASUREMENTS OF SUSCEPTIBILITY

In order to investigate the effect of the interplanar coupling on the magnetic order of $CoCl_2$ GIC's at low tem-

perature, we have performed differential magnetic susceptibility measurements at several fixed temperatures as a function of magnetic field. We applied a probing field of magnitude 0.3 Oe parallel to the finite magnetic in-plane field H_1. The temperature is determined within an error of 2% and the value of H_1 has an error of ± 5 Oe. Despite these relatively large error bars, the general features of the magnetic susceptibility as a function of field are reliable. The details of the experimental setup and measurement technique are described elsewhere,[9] as is the sample characterization.[10]

In Fig. 1, we present the results of the differential magnetic susceptibility as a function of field for several values of the temperature $T \leq 9$ K for a stage-1 $CoCl_2$ GIC sample. We identify two susceptibility peaks as H_{AS} and H_{SF} as indicated on the figure. The susceptibility at a given temperature is for convenience normalized by its maximum value, which occurs in the low-field limit. Since we have presented results for the temperature profile of the susceptibility elsewhere,[7] we concentrate on the field profile in the present paper and assume that the initial values of the susceptibility $[\chi(H \to 0, T)]$ are already established. To interpret the field-dependent results, we plot the locations (H_{AF}, H_{SF}) of the susceptibility peaks as a function of temperature to obtain Fig. 2, which is essentially an experimental phase diagram in the magnetic field-temperature plane, the first phase diagram available for $CoCl_2$ GIC's. We discuss the various phases and their magnetic ordering in the next two sections, where more insight is obtained by the construction of a Landau free-energy functional for our system.

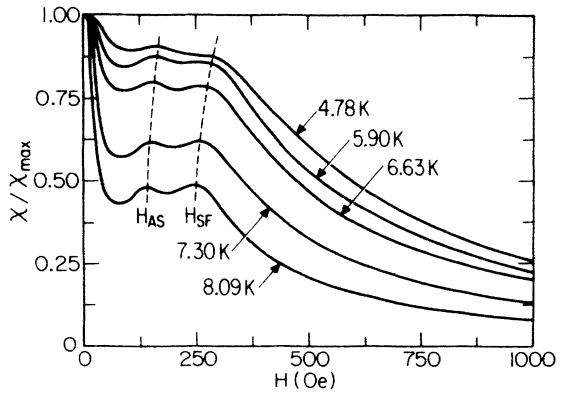

FIG. 1. Differential magnetic susceptibility χ as a function of applied in-plane field H_1 for various temperatures for stage-1 $CoCl_2$ GIC's. The probing field is applied also in the plane of the $CoCl_2$ intercalate, parallel to H_1 and with a magnitude 0.3 Oe. The results are plotted by dividing $\chi(H,T)$ by the maximum value of χ at the same temperature.

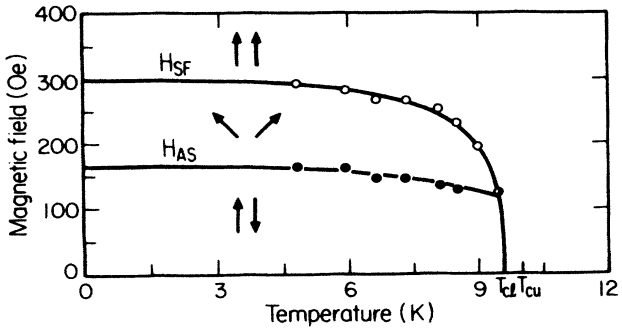

FIG. 2. Experimental phase diagram below T_{cl} obtained by plotting the values of magnetic field corresponding to the two susceptibility peaks in Fig. 1 as a function of temperature. Here the curves labeled H_{AS} and H_{SF} are, respectively, the magnetic field values of the lower and upper field susceptibility peaks in Fig. 1. Between T_{cl} and T_{cu}, the system is in a vortex bound phase in the limit $H \to 0$, and above T_{cu}, the system is in a vortex gas phase in the limit $H \to 0$.

III. LANDAU FREE-ENERGY FUNCTIONAL

The total model Hamiltonian,[5,7,11] consisting of the two-dimensional (2D) XY term, the U_1 and U_p perturbations due to in-plane symmetry-breaking fields and the interplanar antiferromagnetic coupling term, has not been solved exactly. Therefore, we perform a Landau-type analysis of the free energy (see Appendix) to attempt a qualitative understanding of the experimental data for the magnetic field-dependent anomalies. The approach that has been taken is essentially a mean-field-type analysis of the effect of the interplanar coupling, so as to obtain a phase diagram for the system, thereby providing a framework for the interpretation of the magnetic field anomalies.

The Landau free-energy per unit area for one isolated layer of $CoCl_2$ spins consists of three terms: (i) f_{2D} which is the contribution from the ferromagnetic exchange interaction between the XY model spins, (ii) $-\mathbf{H}_1 \cdot \mathbf{M}$ which is the Zeeman interaction of the magnetization $\mathbf{M}$ with the external field $\mathbf{H}_1$, where the units are chosen so that $g\mu_B = 1$, and (iii) $-H_6\rho^6\cos(6\theta)$ which is the sixfold anisotropy energy, where ρ is the magnitude of the magnetization and θ is the angle between the magnetization and an in-plane crystalline axis. From scaling theory in two dimensions, we have the two-dimensional free energy f_{2D} varying with the magnitude ρ of the magnetization according to

$$f_{2D} = c\rho^b , \tag{1}$$

where b is an exponent and c a proportionality constant.

When we consider, in addition, the antiferromagnetic coupling to the nearest-neighboring plane ($J' > 0$) and divide the system into sublattices A and B, we obtain the Landau free energy as

$$\begin{aligned} F_{AB} = {} & f_{2D}^A + f_{2D}^B - H_1\rho_A\cos\theta_A - H_1\rho_B\cos\theta_B \\ & - H_6\rho_A^6\cos(6\theta_A) - H_6\rho_B^6\cos(6\theta_B) \\ & + 2J'\rho_A\rho_B\cos(\theta_A + \theta_B) . \end{aligned} \tag{2}$$

Here ρ_A and ρ_B are the magnitudes of the sublattice magnetization $\mathbf{M}_A$ and $\mathbf{M}_B$ and θ_A, θ_B are their directions with respect to a reference axis. This expression for F_{AB} can be minimized with respect to the quartet of parameters $(\rho_A, \rho_B, \theta_A, \theta_B)$ to obtain the equilibrium configuration. Our first step is to consider the possible equilibrium configuration of F_{AB} at zero temperature and then extend

the analysis to nonzero temperatures by more sophisticated methods.

At zero temperature, we have a system of saturated planar rotator spins lying on successive layers that are coupled antiferromagnetically. Thus, $\rho_A=\rho_B=$const and we can concentrate on the ordering along the direction ($\hat{\mathbf{z}}$ or c) perpendicular to the plane.

This problem is then reduced to the one-dimensional classical antiferromagnetic XY chain with in-plane sixfold anisotropy and an in-plane external field. This one-dimensional problem without in-plane sixfold anisotropy has been investigated by Maki[12] in the soliton language. A similar problem with classical Heisenberg spins, but no sixfold in-plane anisotropy, has been studied using the method of the transfer matrix by Morita and Horiguchi[13] and Lovesey and Loveluck.[14] We will discuss the relevance of the analysis made by these authors[13,14] to our model in the next section.

The zero-temperature analysis, performed by minimizing F_{AB} as a function of θ_A and θ_B, reveals three possible ground states. They are the (i) antiferromagnetic phase: $\theta_A=0$, $\theta_B=\pi$, (ii) spin-flop phase: $0<\theta_A=\theta_B<\pi/2$, and (iii) ferromagnetic (spin-aligned paramagnetic) phase: $\theta_A=\theta_B=0$.

The phase boundaries between these three phases are obtained by comparing the free energies. The antiferromagnetic-spin-flop (A-S) phase boundary for small sixfold anisotropy $g\equiv H_6\rho^6/J'\rho^2$ can be written as

$$h_{\rm AS}=4\sqrt{g} \quad \text{as } g\to 0 , \tag{3}$$

where $h=H_1\rho/J'\rho^2$ and the subscript AS denotes the (A-S) phase transition line. The (A-S) transition is first order since the angle θ changes discontinuously at $h_{\rm AS}$. The phase transition line between the spin-flop phase and the ferromagnetic phase (S-F) for small g can be written as

$$h_{\rm SF}=4-36g \quad \text{as } g\to 0 . \tag{4}$$

To analyze the order of the S-F transition, we follow the method employed by Hornreich, Pension, and Shtrikman.[15] We perform a Taylor expansion of the free energy in the variables θ_A,θ_B around the equilibrium value. The second-order phase transition line is given by the equation

$$\det\mathscr{C}=0 , \tag{5}$$

where $\mathscr{C}=(C_{\mu\nu})$ is the matrix of second-order derivatives of the free energy with $\mu=(A,B)$ and

$$C_{\mu\nu}=\left.\frac{\partial^2 F}{\partial\theta_\mu\partial\theta_\nu}\right|_{\substack{\theta_\mu=\bar{\theta}_\mu\\ \theta_\nu=\bar{\theta}_\nu}} , \tag{6}$$

where $\bar{\theta}_\mu$ and $\bar{\theta}_\nu$ are the equilibrium values.

By the symmetry of the free energy, the third-order derivatives vanish. The transition will then be second order, provided that the fourth-order derivative of the free energy is positive definite. A possible tricritical point will be present if there is a simultaneous solution to $\det\mathscr{C}=0$ and the fourth-order derivative also vanishes at $(\bar{\theta}_A,\bar{\theta}_B)$. We have checked the possibility of a tricritical point for this case and we find that this does not occur in our simple model. Consequently, the S-F transition is always second order in our simple model.

In conclusion, we have found that there are three phases using a stability analysis of the Landau free-energy functional of the antiferromagnetically coupled ferromagnetic XY layers of spins with an in-plane field and sixfold anisotropy. In the next section we will investigate the temperature dependence of the critical fields.

IV. LOW-TEMPERATURE ANALYSIS: TRANSFER-MATRIX METHOD

We use the transfer matrix method to analyze the low-temperature properties of the Landau free energy. We summarize the key steps of the transfer-matrix method before we derive the results for our system.

The transfer-matrix method is useful for one-dimensional statistical mechanics problems of N particles, where the partition function has the form

$$\mathscr{Z}_N=\int d\theta_1\cdots\int d\theta_N e^{-\beta\mathscr{H}(\theta_1,\ldots,\theta_N)} , \tag{7}$$

with $d\theta_i$ as phase space volume element, $\beta=1/k_BT$ and

$$\mathscr{H}(\theta_1,\ldots,\theta_N)=\Psi_I(\theta_N)+\Psi_F(\theta_1)+\sum_{i=1}^{N-1}\mathscr{E}(\theta_i,\theta_{i+1}) . \tag{8}$$

Here, Ψ_I and Ψ_F are the initial state and final state or the end-point spin states of the one-dimensional chain. The quantity $\mathscr{E}(\theta_i,\theta_{i+1})$ is the energy given by

$$\begin{aligned}\mathscr{E}(\theta_i,\theta_{i+1})=&-\tfrac{1}{2}H_1\rho(\cos\theta_i+\cos\theta_{i+1})\\ &-\tfrac{1}{2}H_6\rho^6(\cos6\theta_i+\cos6\theta_{i+1})\\ &+J'\rho^2[\cos(\theta_i-\theta_{i+1})]\end{aligned} \tag{9}$$

for the spin Hamiltonian $\mathscr{H}(\mathbf{S})$ given by

$$\begin{aligned}\mathscr{H}(\mathbf{S})=&J'\sum_{i=1}^{N-1}\rho^2\cos(\theta_i-\theta_{i+1})-\sum_{i=1}^{N}H_1\rho\cos\theta_i\\ &-\sum_{i=1}^{N}H_6\rho^6\cos6\theta_i ,\end{aligned} \tag{10}$$

with $\mathbf{S}_i=\rho(\cos\theta_i,\sin\theta_i)$ being the XY spin in the layer.

The transfer-matrix method involves the integral operator $\mathscr{K}$ defined in the space of the regular function (Ψ) so that

$$\mathscr{K}\Psi(\theta_i)=\int d\theta_{i+1}e^{-\beta\mathscr{E}(\theta_i,\theta_{i+1})}\Psi(\theta_{i+1}) . \tag{11}$$

The partition function $\mathscr{Z}_N$ can be written as

$$\mathscr{Z}_N=\langle\Psi_I^*,\mathscr{K}^{N-1}\Psi_F\rangle \tag{12}$$

with

$$\Psi_I^*(\theta_1)=e^{-\beta\Psi_I(\theta_1)} \tag{13}$$

and

$$\Psi_F(\theta_N)=e^{-\beta\Psi_F(\theta_N)} , \tag{14}$$

and the inner product is defined by

$$\langle g_1^*,g_2\rangle=\int d\theta g_1^*(\theta)g_2(\theta) . \tag{15}$$

The spectrum of the integral operator $\mathscr{K}$ can be shown to have an eigenvalue λ_0 with the smallest absolute value. Denoting Ψ_0 as the normalized eigenstate corresponding to λ_0, we have the free energy f per spin

$$-\beta f=\lim_{N\to\infty}\frac{1}{N}\ln\mathscr{Z}_N=+\ln\lambda_0\ , \tag{16}$$

because $\mathscr{K}\Psi_0=\lambda_0\Psi_0$ with $\langle\Psi_0^*,\Psi_0\rangle=1$.

The problem of finding the free energy for the chain of spins becomes that of finding the smallest absolute eigenvalue λ_0 of the integral operator $\mathscr{K}$. Once λ_0 is found, the magnetization and susceptibility can, in principle, be obtained by successive differentiation with respect to the field H_1.

To obtain the low-temperature properties of the Landau free-energy functional in our competing field model, we can perform a harmonic analysis around the ground state and solve the harmonic integral problem, the lowest eigenvalue of which has an eigenfunction of Gaussian form, thereby allowing analytical computation.

We compute the correction to the spin-flop state as an example. We define the angular deviation from the ground-state spin direction specified by the spin-flop angle θ_0 as

$$\phi_{2n}=\theta_{2n}-\theta_0,\quad \phi_{2n+1}=\theta_{2n+1}+\theta_0 \tag{17}$$

and expand the energy $\mathscr{E}(\theta_{2n},\theta_{2n+1})$ of Eq. (9) to second order in ϕ to get

$$\beta\mathscr{E}(\theta_{2n},\theta_{2n+1})=\beta\mathscr{E}_0(\theta_0)+\beta\frac{\tilde{J}}{2}(\phi_{2n}-\phi_{2n+1})^2+\frac{m^2}{2}(\phi_{2n}^2+\phi_{2n+1}^2)+O(\phi^3)\ , \tag{18}$$

where $\mathscr{E}_0(\theta_0)$ is the ground-state energy given by

$$\mathscr{E}_0(\theta_0)=J'\rho^2\cos(2\theta_0)-H_1\rho\cos\theta_0-H_6\rho^6\cos(6\theta_0)+f_{2D}^A+f_{2D}^B \tag{19}$$

and the new interplanar coupling $\tilde{J}$ and effective mass m are defined by

$$\tilde{J}=-J'\rho^2\cos(2\theta_0)>0\ ,\qquad m^2=\frac{\beta}{2}[H_1\rho\cos\theta_0+H_636\rho^6\cos(6\theta_0)]>0\ . \tag{20}$$

Then, the integral operator equation

$$\int_0^{2\pi}d\phi'\mathscr{K}(\phi,\phi')\Psi_0(\phi')=\lambda_0\Psi_0(\phi) \tag{21}$$

can be solved in the spin-wave approximation by replacing the above equation with

$$e^{-\beta\mathscr{E}_0(\theta_0)}\int_{-\infty}^{\infty}d\phi'\exp\left[-\beta\frac{\tilde{J}}{2}(\phi-\phi')^2-\frac{m^2}{2}(\phi'^2+\phi^2)\right]\Psi_0(\phi')=\lambda_0\Psi(\phi)\ . \tag{22}$$

This is the problem of the harmonic-oscillator kernel[16] which has a solution for Ψ_0 with the Gaussian form

$$\Psi_0(\phi)=ce^{-(m^2/2)\gamma\phi^2}\ , \tag{23}$$

with c and γ as the two parameters fixed by the eigenstate condition [Eq. (21)] and the normalization condition,

$$\int_{-\infty}^{\infty}d\phi\Psi_0^*(\phi)\Psi_0(\phi)=1\ . \tag{24}$$

With two unknowns, c and γ, and two equations, (21) and (24), we can show that

$$\lambda_0=\left[\frac{2\pi}{a_s^2}\right]^{1/2}e^{-\beta\mathscr{E}_0(\theta_0)}\ , \tag{25}$$

where

$$a_s^2=m^2(1+\gamma)+\beta\tilde{J} \tag{26}$$

and

$$\gamma^2=1+\frac{2\beta\tilde{J}}{m^2}\ . \tag{27}$$

After obtaining λ_0, we can compute the free energy f using Eq. (16). The results are summarized in the Appendix. We split the total free energy per spin f into a sum of a zero-temperature contribution f_0 and a low-temperature correction f_1. In the present case of the spin-flop phase, f_0 is $\mathscr{E}_0(\theta_0)$, while f_1 is $(1/2\beta)\ln(a_s^2/2\pi)$. By differentiating the free energy, we obtain the magnetization. The magnetization and the susceptibility are given by

$$M=M_0+M_1,\quad \chi=\chi_0+\chi_1\ , \tag{28}$$

with the zero-temperature magnetization M_0 and susceptibility χ_0 given by

$$M_0=-\frac{d}{dH_1}f_0,\quad \chi_0=-\frac{d^2}{dH_1^2}f_0 \tag{29}$$

and the low-temperature correction terms given by

$$M_1=-\frac{d}{dH_1}f_1,\quad \chi_1=-\frac{d^2}{dH_1^2}f_1\ . \tag{30}$$

In these derivatives, θ_0, m^2, and $\tilde{J}$ are H_1 dependent. The calculations of the magnetization and susceptibility for the other two phases are similar and the results are summarized in the Appendix.

The value of χ as a function of h ($\equiv H_1\rho/J'\rho^2$) is plotted for fixed six-fold anisotropy g ($\equiv H_6\rho^6/J'\rho^2$) in Figs. 3(a), 3(b), and 3(c), corresponding to the antiferromagnetic ground state, the spin-flop ground state, and the ferromagnetic (spin-aligned paramagnetic) ground state, respectively. For these curves, the temperature scale is set by $\beta\tilde{J}=100$ and χ is normalized by setting $\chi_{\max}=1$ for

each phase. These curves provide a qualitative picture of the observed field-induced anomalies.

In the antiferromagnetic phase [Fig. 3(a)], the susceptibility first decreases and then increases. These curves terminate at certain specific values $h(g)$ for a given g, because the harmonic approximation around the antiferromagnetic ground state breaks down for higher values of h. In Fig. 3(a) we see that the termination value $h(g)$ is smaller for smaller g values. This indicates that the phase transition from the antiferromagnetic state to the spin-flop state occurs at a critical field $h_{AS}=h_c(g)\geq h(g)$, such that $h_c(g)$ increases with increasing g values, according to the harmonic approximation. A second point to note in Fig. 3(a) is that near $h(g)$, the harmonic approximation

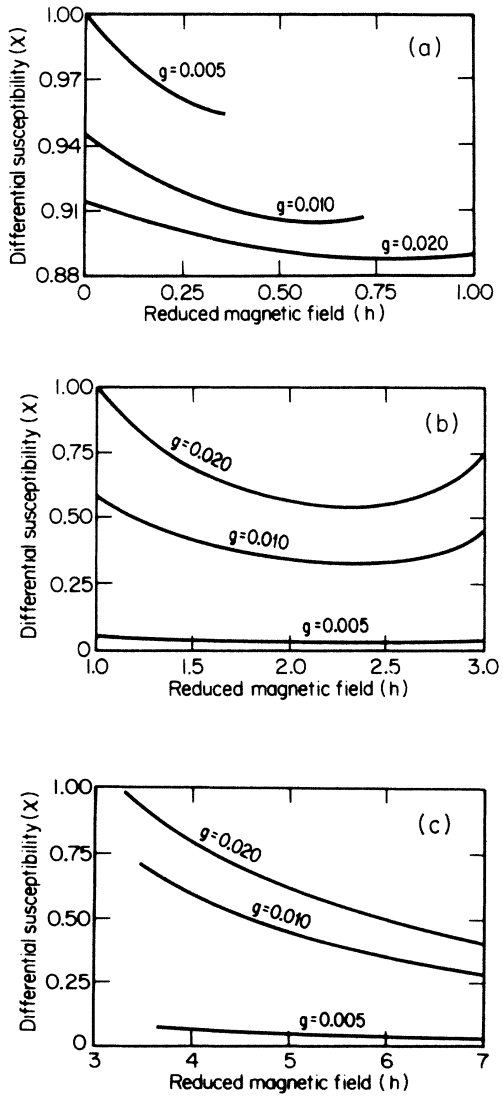

FIG. 3. Differential magnetic susceptibility versus reduced field in the (a) antiferromagnetic, (b) spin-flop, and (c) ferromagnetic (spin-aligned paramagnetic) phase for various fixed values of the sixfold anisotropy $g\equiv H_6\rho^6/J'\rho^2$. In (a) the curves are terminated at field values where the harmonic approximation breaks down. Likewise, in (c) the curves start at fixed values where the harmonic approximation becomes valid. Close to h_{AS} and h_{SF} the harmonic approximation breaks down.

fails, since the susceptibility should diverge at $h_c(g)$. Beyond $h_c(g)$, the system is in the spin-flop state. The harmonic-approximation calculation for χ around the spin-flop ground state is shown in Fig. 3(b). Although the values of g used in these plots are for illustrative purposes only, it should be noted that in Figs. 3(a) and 3(b) the magnitude of χ in Fig. 3(a) increases as g decreases, but the reverse is true in Fig. 3(b). This can be explained by the following physical argument. If in the antiferromagnetic state g goes to zero, then the spin-flop transition occurs at zero h. This is the familiar case where the application of a field will flop the antiferromagnetically ordered spins in the direction perpendicular to the field. Because of the sixfold anisotropy, this spin-flop process is more difficult. On the average, the sixfold anisotropy g presents each spin and its antiferromagnetic neighbors with a stiffness, over which the spins must flop; the free-energy barrier is larger, the larger the value of $H_6\rho^6$; thereby, the smaller the response, and the smaller the susceptibility. On the other hand, in the spin-flop (or ferromagnetic) state, the antiferromagnetic coupling $J'\rho^2$ plays the role $H_6\rho^6$ plays in the antiferromagnetic state. $J'\rho^2$ provides the stiffness for the spins to rotate towards the external-field direction. Since g is defined as $H_6\rho^6/J'\rho^2$, the response and thus the susceptibility is larger, the smaller the value of $J'\rho^2$, or the larger the value of g. In Fig. 3(c) we see that the values of χ can be calculated only for those values of h where $h\geq\tilde{h}(g)$ and $\tilde{h}(g)$ is an estimate of h_{SF} by the harmonic approximation. This situation is essentially the same as the one illustrated in Fig. 3(a). In Fig. 3(c) the harmonic approximation around the ferromagnetic ground state is not possible for $h<\tilde{h}(g)$. The correct harmonic approximation for $h<\tilde{h}(g)$ should be made using the spin-flop ground state [Fig. 3(b)].

We now discuss the connection between the susceptibility curves of Figs. 3(a), 3(b), and 3(c) for each phase. Since the susceptibility diverges at the critical fields h_{AS} and h_{SF}, the exact values of the susceptibility in Figs. 3(a), 3(b), and 3(c) cannot be determined and only their relative values have meaning. Thus, the overall picture derived from Figs. 3(a), 3(b), and 3(c) is the following: at very small h values, χ decreases then increases as h approaches h_{AS} from below and then diverges at h_{AS}, where the system goes through a phase transition from the antiferromagnetic to the spin-flop phase; in the spin-flop phase, χ decreases as h approaches h_{AS} and eventually increases without limit as h approaches h_{SF}, where the system goes through a transition from the spin-flop state to the ferromagnetic state; in the ferromagnetic state, χ decreases monotonically with increasing h. It is this general picture that is provided by the harmonic approximation using the transfer-matrix method. A quantitative comparison of theory and the experimental data requires much more detailed analysis.

V. DISCUSSION

The field-induced anomalies in the susceptibility of $CoCl_2$ GIC's allow the determination of the first experimental phase diagram of $CoCl_2$-intercalated graphite. A simple theory using Landau's approach can account for

the qualitative features exhibited by these anomalies by focusing on the c-axis ordering. It is a success of the theory that these anomalies were first predicted by the theory and later confirmed by experiments. Similar experiments were carried out concurrently on stage-2 $NiCl_2$ GIC's by Suzuki and Ikeda.[17] The observed field-induced anomalies indicate that a two-dimensional spin-flop transition takes place at H_{AS}, and another transition from a spin-flop phase to a ferromagnetic phase occurs at $H_{SF} > H_{AS}$. The 2D spin-flop phase is new in the sense that the ferromagnetic XY interplanar coupling is large, forbidding the conventional 3D spin-flop transition, where the spin in a field will flop over to the direction perpendicular to the field. In the 2D case discussed here, the spins in one plane make an angle θ with respect to the spins in the adjacent plane. This behavior is a result of the sixfold in-plane symmetry-breaking field, since H_6 creates the necessary stiffness to counter the tendency of spins to flop towards the direction perpendicular to the field. A qualitative understanding of this novel phase in a two-dimensional magnetic system is summarized in Fig. 4. When $H_6=0$ (no sixfold anisotropy), the application of a small external field will flop the spins that are originally antiparallel along the x direction towards the y direction by first canting the antiparallel pair. This is in contrast to the case where $H_6 \neq 0$ and the flopping of the spins does not occur until $H_1 > H_{AS}$. As shown in Fig. 4, the sixfold anisotropy favors the near 60° angular alignment, rather than the near 90° angular order. The flopping of the spins out of plane is energetically unfavorable since the in-plane ferromagnetic exchange J is very large (in the tesla range) compared to J', H_6, or H_1 (in the oersted range). It would be interesting to look for this

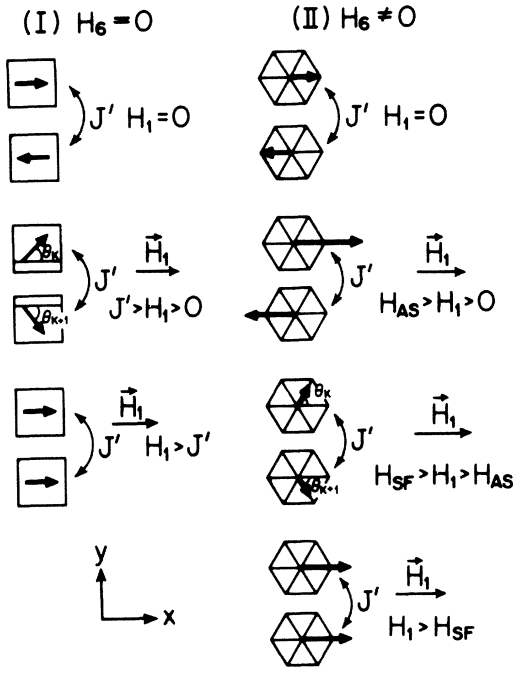

FIG. 4. Schematic representation of the two-dimensional spin-flop transition. (Refer to discussion in Sec. V.)

out-of-plane spin flop at high magnetic fields. Since the magnetic susceptibility measures the response of the system to an external field, we expect another peak in χ at a field of the order of the intraplanar coupling.

The identification of the fields where the susceptibility is a maximum with the critical fields follows from the mathematical analysis of the Landau free energy. Physically, this is also easy to understand since χ, the magnetic response of the system to the external field, is largest near the phase transition point.

To obtain an estimate of the parameters of the model, we first extrapolate the experimental critical fields at nonzero temperature, assuming that there is no new phase transition. For the stage-1 $CoCl_2$-GIC samples, we obtain values for H_{AS} and H_{SF} in the neighborhood of 160 and 300 Oe, respectively (see Fig. 1).

We now compare these values with the theoretical predictions. We assume that the value of the sixfold anisotropy is much smaller than the interplanar coupling, so that we can make use of Eqs. (3) and (4), where h_{AS} and h_{SF} are given by $4\sqrt{g}$ and $4-36g$, respectively. According to the experimental data, the extrapolated critical fields at zero temperature can be used for the comparison with the theoretical prediction, as given by the following equation:

$$\frac{H_{AS}}{H_{SF}} = \frac{4\sqrt{g}}{4-36g} = \frac{160\pm 10 \text{ Oe}}{300\pm 10 \text{ Oe}} . \tag{31}$$

The value of g found in this equation is 0.06 ± 0.01. Consequently, the values of h_{AS} and h_{SF} can be obtained. From the definition of g and h, we obtain the approximate values of J' and H_6 as $J'=160\pm 30$ Oe (1.07×10^{-2} K) and $H_6=10\pm 2$ Oe (6×10^{-4} K), respectively, for stage-1 $CoCl_2$ GIC's.

These estimates of the interplanar coupling and sixfold in-plane anisotropy are consistent with the estimates of Suzuki *et al.*[8] using neutron scattering ($J'/J \sim 10^{-4}$ and $H_6 \approx 10$ to 20 Oe) and by Karimov and co-workers[18–20] ($10 < H_6 < 30$ Oe). It should be noted that Suzuki's estimate is for a stage-2 compound so that J' for the stage-1 compound is expected to be larger. Correspondingly, we do not expect any significant stage dependence for H_6. Furthermore, the present analysis gives $J'/J = 3.8\times 10^{-4}$, in agreement with the results from the analysis of the temperature profile of the susceptibility ($J'/J = 4\times 10^{-4}$), using the theory of the finite-size generalized JKKN model[5,21] with the Liu-Stanley correction[22] for the interplanar coupling.

From the above discussion, we have shown that the analysis of the field profile of the susceptibility of $CoCl_2$ GIC's allows us to obtain the best values to date for the interplanar coupling and the in-plane sixfold anisotropy. By reducing the experimental error in our measurements and extending the measurements towards lower temperatures, we can obtain a better understanding of the phase diagram as well as better values for J'/J and H_6. However, the theoretical model developed in this paper oversimplifies the actual system, insofar as the existence of crystallites and finite intercalant islands requires a model that takes into account the angular dependences of the applied in-plane field with respect to the sixfold axis. An analysis

of this complication has been carried out for the case of the pure two-dimensional model,[23,24] where the competition effect of the sixfold field and the external field is investigated at low temperatures. These extensions of the model can also be carried out using the Monte Carlo method.

Finally, a most interesting area for future research on $CoCl_2$ GIC's is the study of multicritical phenomena by considering competing interactions along the c axis. Such effects could involve the occurrence of Lifshitz points. In this context, the experimental refinement of the phase diagram (Fig. 2) around the triple point will be extremely fruitful.

ACKNOWLEDGMENTS

We are grateful to Professor M. S. Dresselhaus, Professor P. A. Lee, Professor A. N. Berker, and Professor J. V. José for their helpful comments. This work was supported by U.S. Air Force Office of Scientific Research Contract No. F49620-83-C0011. K. Y. Szeto acknowledges the support of Natural Sciences and Engineering Research Council of Canada and of the Imperial Oil Company of Canada. S. T. Chen acknowledges support from IBM.

APPENDIX

In this Appendix we summarize the expressions for the free energy $f=f_0+f_1$ using the transfer-matrix method, where f_0 is the zero-temperature free energy and f_1 is the correction term at low temperatures. The ferromagnetic ground state has the following expressions:

$$f_0=f_{2D}+J'\rho^2-H_1\rho-H_6\rho^6,\quad f_1=\frac{1}{2\beta}\ln\left[\frac{a_f^2}{2\pi}\right], \tag{A1}$$

in which

$$a_f^2=m^2(\gamma+1)-\beta\tilde{J},\quad m^2=\tfrac{1}{2}\beta(H_1\rho+36H_6\rho^6),$$
$$\tilde{J}=-J'\rho^2,\quad \gamma^2=1+\frac{2\beta\tilde{J}}{m^2}. \tag{A2}$$

The spin-flop ground state has free-energy expressions

$$f_0=f_{2D}+J'\rho^2\cos(2\theta_0)-H_1\rho\cos\theta_0-H_6\rho^6\cos(6\theta_0), \tag{A3}$$
$$f_1=\frac{1}{2\beta}\ln\frac{a_s^2}{2\pi},$$

in which

$$a_s^2=m^2(\gamma+1)+\beta\tilde{J},$$
$$m^2=\frac{\beta}{2}[H_1\rho\cos\theta_0+36H_6\rho^6\cos(6\theta_0)], \tag{A4}$$
$$\tilde{J}=-J'\rho^2\cos(2\theta_0),\quad \gamma^2=1+\frac{2\beta\tilde{J}}{m^2}.$$

The antiferromagnetic ground state has free-energy expressions

$$f_0=f_{2D}+J'\rho^2+H_6\rho^6,\quad f_1=\frac{1}{2\beta}\ln\left[\frac{A_+A_-}{2\pi}\right], \tag{A5}$$

in which

$$A_\pm^2=\beta\tilde{J}[1+X_\pm(1+\gamma_\pm)],\quad X_\pm=\frac{m^2}{\beta\tilde{J}}\pm\frac{\beta}{2}\left[\frac{H_1\rho}{\beta\tilde{J}}\right],$$
$$\tilde{J}=J'\rho^2,\quad m^2=\frac{\beta}{2}(36H_6\rho^6) \tag{A6}$$
$$\gamma_\pm^2=\frac{1}{X_\pm^2}\left[(1+X_\pm)^2-\frac{(1+X_\pm)}{(1+X_\mp)}\right].$$

[1]Y. Shapira and S. Foner, Phys. Rev. B **1**, 3083 (1970).
[2]H. Rohrer and Ch. Gerber, Phys. Rev. Lett. **38**, 909 (1977).
[3]R. M. Hornreich, M. Luban, and S. Shtrikman, Phys. Rev. Lett. **35**, 1678 (1975).
[4]R. M. Hornreich, J. Magn. Magn. Mater. **15-18**, 387 (1980).
[5]K. Y. Szeto, Ph.D. thesis, Massachussetts Institute of Technology, 1985.
[6]J. V. José, L. P. Kadanoff, S. Kirkpatrick, and D. R. Nelson, Phys. Rev. B **16**, 1217 (1977).
[7]K. Y. Szeto, S. T. Chen, and G. Dresselhaus, Phys. Rev. B **32**, 4628 (1985).
[8]M. Suzuki, H. Ikeda, and Y. Endoh, Synth. Met. **C8**, 43 (1983).
[9]M. Elahy and G. Dresselhaus, Phys. Rev. B **30**, 7225 (1984).
[10]S. T. Chen, K. T. Szeto, M. Elahy, and G. Dresselhaus, J. Chim. Phys. **81**, 863 (1984).
[11]K. Y. Szeto, S. T. Chen, G. Dresselhaus, and M. S. Dresselhaus, *Proceedings of the 17th International Semiconductor Conference*, edited by J. A. Chadi and W. A. Harrison (Springer, New York, 1984), p. 969.
[12]K. Maki, J. Low Temp. Phys. **41**, 2 (1980).
[13]T. Morita and T. Horiguchi, Physica **83A**, 519 (1976).
[14]S. W. Lovesey and J. M. Loveluck, J. Phys. C **9**, 3639 (1976).
[15]R. M. Hornreich, K. A. Penson, and S. Shtrikman, J. Phys. Chem. Solids **33**, 433 (1972).
[16]R. P. Feynmann and A. R. Hibbs, *Path Integrals and Quantum Mechanics* (Academic, New York, 1968).
[17]M. Suzuki and H. Ikeda, J. Phys. C **14**, L923 (1981).
[18]Yu. Karimov, M. E. Vol'pin, and Y. Novikov, Zh. Eksp. Teor. Fiz. Pis. Red. **14**, 217 (1971) [Sov. Phys.—JETP Lett. **14**, 142 (1971)].
[19]Yu. Karimov, Zh. Eksp. Teor. Fiz. **66**, 1121 (1974) [Sov. Phys.—JETP **39**, 547 (1974)].
[20]Yu. Karimov, Zh. Eksp. Teor. Fiz. **68**, 1539 (1975) [Sov. Phys.—JETP **41**, 772 (1976).
[21]K. T. Szeto and G. Dresselhaus, Phys. Rev. B **32**, 3142 (1985).
[22]L. L. Liu and H. E. Stanley, Phys. Rev. B **8**, 2279 (1973).
[23]K. Y. Szeto and G. Dresselhaus, J. Phys. C (to be published).
[24]K. Y. Szeto and G. Dresselhaus, Phys. Rev. B **32**, 3186 (1985).